

AD-A192 072

INJECTION OF DRAG REDUCING ADDITIVES INTO TURBULENT
WATER FLOWS(U) PURDUE UNIV LAFAYETTE IN SCHOOL OF
MECHANICAL ENGINEERING D T WALKER ET AL. FEB 88

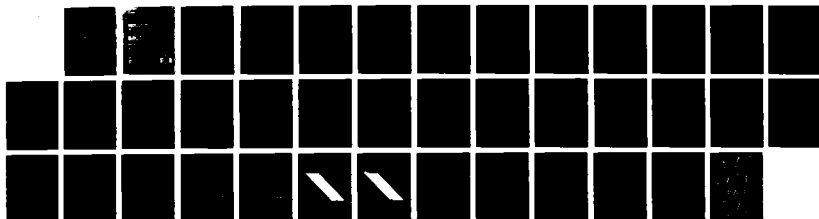
1/1

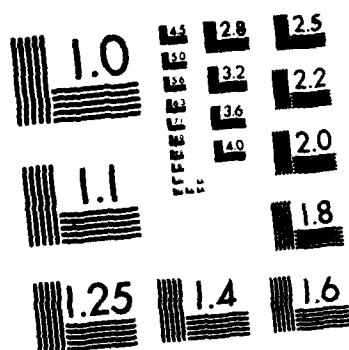
UNCLASSIFIED

PME-FH-88-1 N00014-83-K-0183

F/G 20/4

NL





MICROCOPY RESOLUTION TEST CHART
NATIONAL BUREAU OF STANDARDS 1963-A

4

AD-A192 072

REDUCTION OF DRAG REDUCING ADDITIVES INTO TURBULENT WATER FLOWS

Quantitative Results from Time-Resolved Measurements

David T. Walker and William G. Tiederman
School of Mechanical Engineering
Purdue University
West Lafayette, Indiana 47907

February, 1988

Technical Report for Period 01 March 1987 - 30 November 1987

Approved for public release; distribution unlimited

Prepared for

OFFICE OF NAVAL RESEARCH
900 North Quincy Street
Arlington, VA 22217-5000


DTIC
ELECTE
S MAR 01 1988 D
H

88 2 29 120

REPORT DOCUMENTATION PAGE		READ INSTRUCTIONS BEFORE COMPLETING FORM
1. REPORT NUMBER PME-FM-88-1	2. GOVT ACCESSION NO.	3. RECIPIENT'S CATALOG NUMBER
4. TITLE (and Subtitle) INJECTION OF DRAG REDUCING ADDITIVES INTO TURBULENT WATER FLOWS: Concentration Measurements from Time-Resolved Measurements		5. TYPE OF REPORT & PERIOD COVERED Technical Report for March 1, 1987 through November 30, 1987
7. AUTHOR(s) David T. Walker, William G. Tiederman		6. PERFORMING ORG. REPORT NUMBER
9. PERFORMING ORGANIZATION NAME AND ADDRESS School of Mechanical Engineering Purdue University West Lafayette, IN 47907		8. CONTRACT OR GRANT NUMBER(s) N00014-83K-0183
11. CONTROLLING OFFICE NAME AND ADDRESS Office of Naval Research 800 North Quincy Street Arlington, VA 22217-5000		10. PROGRAM ELEMENT, PROJECT, TASK AREA & WORK UNIT NUMBERS 4322-754
14. MONITORING AGENCY NAME & ADDRESS (if different from Controlling Office)		12. REPORT DATE February 1988
		13. NUMBER OF PAGES 32
		15. SECURITY CLASS. (of this report)
		15a. DECLASSIFICATION/DOWNGRADING SCHEDULE
16. DISTRIBUTION STATEMENT (of this Report) APPROVED FOR PUBLIC RELEASE: DISTRIBUTION UNLIMITED		
17. DISTRIBUTION STATEMENT (of the abstract entered in Block 20, if different from Report)		
18. SUPPLEMENTARY NOTES		
19. KEY WORDS (Continue on reverse side if necessary and identify by block number) Drag reduction; turbulent wall flows; concentration measurement		
20. ABSTRACT (Continue on reverse side if necessary and identify by block number) The primary objective of this portion of the program is to build a data base that is sufficient to critically test models of the initial mixing between a polymer solution injected at the wall and a turbulent water flow. Time-resolved concentration measurements were made using a laser-induced fluorescence technique downstream of a flush mounted wall injector. The injected polymer solution was a 700 ppm aqueous solution of SEPARAN AP-273. For comparison purposes, measurements were also made for a water injection at		

(Continued)

the same flow rate.

The results for the instantaneous, mean and root-mean-square concentration profiles at positions 10, 25, 50 and 100 mm downstream of the injector show how the mixing decreases when the injectant is a polymer solution. 

CONTENTS

INTRODUCTION	1
APPARATUS AND PROCEDURES	4
2.1 Experimental Facilities	4
2.2 Concentration Measurements	7
2.2.1 Analysis	7
2.2.2 Data Acquisition	10
2.2.3 Optical Arrangement	11
2.2.4 Concentration Measurement Procedure	12
RESULTS	14
3.1 Mean Concentration Profiles	15
3.2 Root-Mean-Square Concentration Profiles	18
3.3 Time-Resolved Concentration Profiles	22
CONCLUSIONS	29
REFERENCES	30
DISTRIBUTION LIST	31



Accession For	
NTIS GRA&I	<input checked="" type="checkbox"/>
DTIC TAB	<input type="checkbox"/>
Unannounced	<input type="checkbox"/>
Justification	
By	
Distribution/	
Availability Codes	
Dist	Avail and/or Special
A-1	

LIST OF SYMBOLS

<i>Symbol</i>	<i>Description</i>
A_n	calibration constant for photodiode element n
C	instantaneous concentration
C_i	initial concentration of injected fluid
I	fluorescence intensity
I_e	intensity of excitation laser beam
I_0	initial laser intensity
V_n	measured voltage for photodiode element n
V_{dn}	dark-level voltage for photodiode element n
a_n	fraction of total fluorescent emission incident on photodiode element n
b_n	sensitivity of photodiode element n
c	concentration fluctuation, $c = C - \bar{C}$
d	length of concentration measurement volume in direction normal to the wall
h	channel height
k	extinction coefficient for dye
s	spacing of concentration measurement volumes in direction normal to the wall

u_r	shear velocity, $u_r = \sqrt{\tau_w/\rho}$
x	streamwise distance measured from injector
y	distance from wall
α	proportionality constant relating the fluorescent emission of the dye to the amount of light absorbed
β	proportionality constant relating the dye extinction coefficient to the dye concentration
ν	kinematic viscosity
ρ	density
τ_w	wall shear stress

Superscripts

+	normalized with inner variables u_r and ν
-	time average
'	root mean square (RMS)

Subscripts

w	pertains to water flow
---	------------------------

INTRODUCTION

The basic goals of this project are: (1) to determine the mechanisms by which drag-reducing additives injected at the wall in a turbulent channel flow modify the turbulent transport; and (2) to build a data base that can be used to critically test models of the high Schmidt number turbulent mixing process between an injected drag-reducing polymer solution and the water flow. The purpose is to develop methods for predicting, controlling and manipulating turbulent wall flows.

The addition of small amounts of soluble, high molecular weight polymer molecules to water flows has been one of the most successful methods for reducing drag and manipulating near-wall turbulent structures. This project is concerned with injection of low concentration (less than 0.2 percent) polymer solutions through flush-mounted, angled wall slots into fully developed channel flows (see Walker et al., 1986). In the region just downstream of the slot, the modifications to the flow and the performance of the injected solution as a drag reducer will depend on the mixing of the polymer with the ambient fluid.

Although the evolution of the mean polymer concentration profile downstream of wall injectors has been investigated by various authors, the nature of the mass transfer processes that govern this evolution have not been examined directly. The Schmidt number for diffusion of polymer solutions in water is high (> 1000) hence, mass transfer is dominated by turbulent transport mechanisms. Since turbulent mass transfer is convective in nature and the polymer is not a passive scalar (i.e. the turbulence is modified locally by the polymer), mass and momentum transport

downstream of an injector are coupled. In order to model this type of flow without ad-hoc assumptions, measurements of turbulent mass transport and momentum transport are necessary.

Investigations into the mixing of injected polymer solutions have been limited to the measurement of mean concentration profiles. Latto and El Reidy (1976,1984) measured mean concentration profiles downstream of slot injectors in a flat plate boundary layer and showed that polymer solutions diffuse more slowly than water solutions. An investigation by Collins and Gorton (1976) showed that downstream of the region where large concentration gradients exist, diffusion rates are comparable to those resulting from plain water injection. Fabula and Burns (1970) measured the mean polymer concentration profile far downstream of a slot injector in a zero pressure gradient boundary layer. They showed that in this region, where the polymer was present across the entire boundary layer, the concentration profile was self-similar.

All these measurements were made using pitot probes and isokinetic sampling techniques. Latto et al. (1981) have shown that measured mean concentrations are always less than actual concentrations in inhomogeneous flows when this measurement technique is used due to the strong concentration dependence of the solution's viscosity.

None of the above mentioned studies examine the concentration in the near-field, the region just downstream of the injector where large concentration gradients exist and the polymer solution begins to modify the flow.

The study of Walker and Tiederman (1987) examined the near-field evolution of the mean concentration profile in a turbulent channel flow and its effect on the long-time averaged turbulent structure. They found that at a location four channel heights (100 mm) downstream of the injector, the near-wall turbulent structure had been modified and that for distances greater than four channel heights the structure had been altered across the entire flow. This indicated that the initial interaction between the polymer solution and the flow occurred in the first 100 mm downstream of the injector.

In the past nine months, a laser-induced fluorescence technique has been implemented which allows non-intrusive measurements of time-resolved injectant concentration profiles in the region near the injector. To this end, a Masscomp 5520 micro-computer was interfaced with a Reticon line-scan camera. The Masscomp computer features a large random-access memory and fast analog to digital conversion capability required for the concentration measurement technique. It was used for timing, data acquisition and data analysis. Concentration measurements were successfully made downstream of the injector for injection of both a polymer solution and, for purposes of comparison, pure water.

APPARATUS AND PROCEDURES

2.1 Experimental Facilities

The water flow loop used in these experiments, shown in Figure 1, was driven by four ninety gallon per minute centrifugal pumps operating in parallel. The maximum Reynolds number, based on channel height, for this loop was in excess of 40,000. At each end of the test section there was a large stilling tank to isolate the test section from any hydrodynamic disturbances in the flow loop. The upstream stilling tank contained a perforated plate followed by a screen and open-cell sponge section and a smooth two-dimensional contraction leading to a rectangular cross section. The inlet of the channel was preceded by a flow straightener consisting of closely packed plastic drinking straws which insured that no large-scale vorticity existed in the channel entry flow. The downstream tank contained a perforated plate to damp out disturbances and a copper coil through which cooling water flowed to maintain the channel water at a constant temperature.

The flow loop had a rectangular cross-section channel (6.0 cm high by 57.5 cm wide) as the test section. The test section was constructed from one half inch acrylic and polycarbonate sheet and was more than one hundred channel heights long. Polymer solutions were injected through flush-mounted, angled slots located in both of the 57.5 cm walls of the channel. The injection slots had a width, measured in the streamwise direction, of 2.5 mm and were inclined 25 degrees to the flow direction as shown in Figure 2. The injectors were located about eighty channel heights downstream of the inlet.

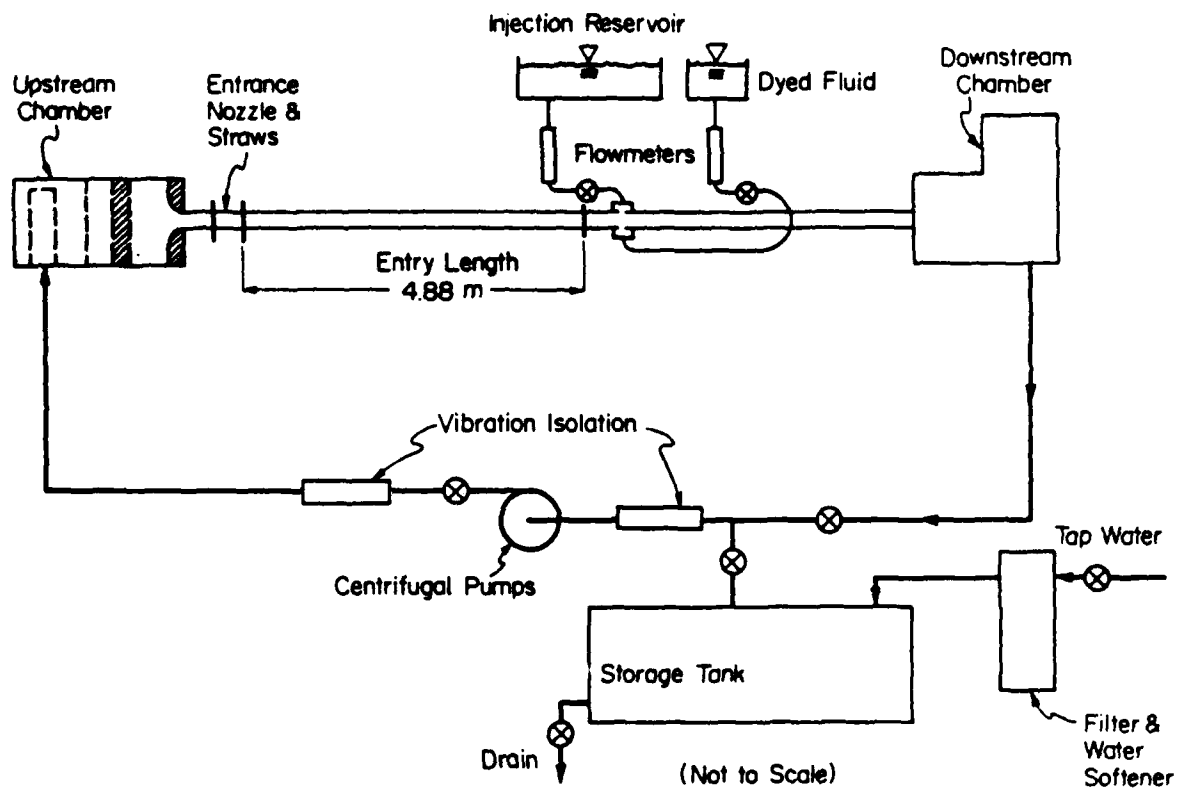


Figure 1 Schematic of flow loop.

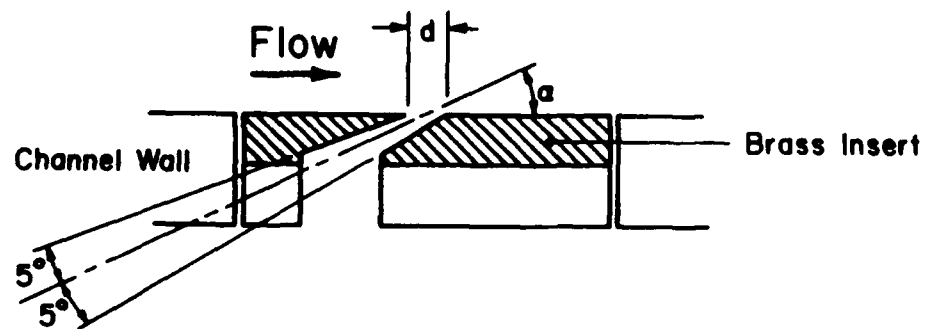


Figure 2 Section view of injection slot; $d=2.5\text{mm}$, $\alpha = 25$ degrees.

2.2 Concentration Measurements

Time-resolved concentration measurements were obtained in a manner similar to that used by Koochesfahani and Dimotakis (1986). The injected fluid was marked with a fluorescent dye and the spatial distribution of the intensity of fluoresced light emitted from a laser beam directed normal to the channel wall was measured. The dye concentration at a point was determined from the fluorescent light intensity and the injectant concentration was inferred from the measured dye concentration. For turbulent flows, where dispersion occurs due to convective mixing, the "turbulent" mass diffusivity is typically two or more orders of magnitude larger than the molecular mass diffusivity. This indicates that the time scale for molecular diffusion is more than one hundred times the timescale for "turbulent diffusion", hence the effect of molecular diffusion will be small and the tracer concentration will yield a good estimate of the polymer concentration.

2.2.1 Analysis

For light propagating in an absorbing medium, e.g. a laser beam propagating through a fluorescent dye, the intensity at any point, y , along the path is given by

$$I_e(y) = I_0 \exp \int_0^y -k(r) dr \quad (1)$$

where I_0 is a reference intensity (at y equal zero) and k is the extinction coefficient for the medium. The intensity of the fluoresced light, I , emitted from a small length of the excitation beam extending from $y-d/2$ to $y+d/2$ is some fraction of the light absorbed over that distance. Hence, for small d

$$I(y) = I_e(y-d/2)\alpha k(y)d \quad (2)$$

where α is a constant, y denotes a position at the center of the segment of length d from which the fluoresced light is emitted and k is the average extinction coefficient over that segment. For fluorescent dyes in the range of concentrations of interest here, the extinction coefficient is proportional to the dye concentration

$$k = \beta C. \quad (3)$$

Combining the above equations yields

$$I(y) = I_o \alpha \beta C(y) d \exp \int_0^{y-d/2} -\beta C(r) dr. \quad (4)$$

This equation relates the fluorescence intensity at a point along the path of the laser beam to the incident intensity and the dye concentration along the beam path. Solving for the local concentration $C(y)$ yields

$$C(y) = \frac{I(y)}{I_o \alpha d} \exp \int_0^{y-d/2} \beta C(r) dr. \quad (5)$$

If the dye concentration is considered constant over a distance s measured from the midpoint between segments $i-1$ and i to the midpoint between segments i and $i+1$, then the integration in the above equation can be written as a summation and the average dye concentration over the n th segment, $C(y_n) = C_n$, is given by

$$C_n = \frac{I_n}{I_o \alpha \beta d} \exp \sum_{i=1}^{n-1} \beta C_i s. \quad (6)$$

This result can be rewritten as

$$C_n = \frac{I_n}{I_o \alpha \beta d} \prod_{i=1}^{n-1} \exp \beta C_i s. \quad (7)$$

This last equation expresses the dye concentration at the n th location along the beam path in terms of the properties of the dye, the dye concentration at the previous $n-1$

locations, and the intensity of the fluorescent emission from a small segment of the excitation beam. Also required are the values of d and s which are determined by the detector used for the fluorescence intensity measurements.

For these experiments the fluorescence intensity distribution along the path of the excitation laser beam was measured using a Reticon camera incorporating a line array of photodiodes. In developing working equations, the characteristics of the photodiode array and the imaging optics must be considered. The voltage for a given element of the array increases linearly with incident light intensity from a dark-level voltage. Both the dark-level voltage and the sensitivity vary slightly from element to element. In addition, since measurements were made near a wall, the fraction of the total fluorescent emission collected by the camera lens varied with position in the field of view.

The voltage for a given element is related to the fluorescent intensity at the corresponding point in the field of view by

$$V_n = \frac{I_n}{a_n b_n} + V_{dn} \quad (8)$$

where a_n is the fraction of the emitted light which is incident on the element, b_n is the sensitivity of the element and V_{dn} is the dark voltage for the element. Combining this result with equation (7) yields

$$C_n = (V_n - V_{dn}) \left[\frac{a_n b_n}{I_o \alpha \beta d} \right]^{n-1} \prod_{i=1}^{n-1} \exp \beta C_i s \quad (9)$$

which relates concentration to measured voltage. Examination of this equation reveals that the term in brackets depends entirely on known constants and element number. Hence, this term can be replaced by a single variable A_n , resulting in

$$C_n = \frac{1}{A_n} \left[\prod_{i=1}^{n-1} \exp \beta C_i s \right] (V_n - V_{dn}). \quad (10)$$

The single element-dependent constant is then determined by placing a known dye concentration in the flow field and measuring the array element voltages.

2.2.2 Data Acquisition

All timing and data acquisition tasks were accomplished using a Masscomp 5520 micro-computer. Data were acquired using an 12 bit A/D converter capable of one million conversions per second and all timing was controlled by a set of on-board clocks. This computer has 10 Mbytes of random access memory (approximately 8 Mbytes available for data acquisition) and a 71 Mbyte hard disk. Data and programs can be archived off-line using a 1/4 in. cartridge tape drive (55 Mbytes per tape). The computer has sufficient hardware floating point calculation capability and graphics capability to analyze data on-line during the course of an experiment.

The Reticon line-scan camera requires a clock pulse to start each scan of the array and a clock signal to drive the multiplexer which samples the individual elements. The frequency at which scans of the array are started will be referred to as the scan rate; the frequency of the signal used to drive the multiplexer will be called the clock rate. These timing signals can be either supplied externally or generated within the camera. The output signal from each element is in the form of a dark-level voltage plus a voltage proportional to the integrated intensity of the light incident on the element during the time between successive scans of the array. Hence, the rate at which the array is scanned defines the exposure time for each intensity profile. The maximum output voltage is two volts and the dark level voltage is about 10 mV.

In order to synchronize the camera timing with the data acquisition all timing signals were generated using the CK10 clock module of the Masscomp computer. For all measurements presented here the camera was clocked at 857 kHz. For long-time averaged statistics the array scan rate was 3 kHz yielding an exposure time of 333 microseconds. Every sixth scan of the array was digitized resulting in a sampling rate of 500 Hz and 10,000 concentration profiles were stored., For time-resolved measurements the array was scanned at a rate of 2 kHz for an exposure time of 500 microseconds, each scan of the array was digitized resulting in a sampling rate of 2 kHz and 4,000 concentration profiles were stored.,

These data were acquired using the AD12FA analog to digital converter which has eight differential channels and can be programmed for gains between one and 64. This device is capable of one million conversions per second at a gain of one and 900,000 conversions per second at a gain of four. Since the maximum camera signal was two volts, the A/D was set for a gain of four.

2.2.3 Optical Arrangement

For these experiments the fluorescence intensity distribution along the path of the excitation laser beam was measured using a Reticon line-scan camera incorporating a 256 element, self-scanning linear photodiode array. The elements of the photodiode array are 25 μm by 425 μm and are located on 50 μm centers. With magnification, this resulted in effective measurement volumes 30.3 μm in the direction normal to the wall spaced 60.5 μm apart.

The blue (488 nm) line from a Lexel model 85.5 argon ion laser was used to

excite the dye. The diameter of the excitation beam determined the spatial resolution of the measurement in the streamwise and spanwise directions. Focusing the excitation beam with a 200 mm focal length lens yielded a beam diameter of about 110 μm across the entire field of view.

2.2.4 Concentration Measurement Procedure

Prior to the concentration measurements the injected fluid was dyed at a concentration of one to two parts per million with fluorescein disodium salt. The water in the flow loop was given a dye concentration of 0.1 to 0.2 ppm of fluorescein for purposes of calibration. The camera was positioned and aligned visually with the excitation beam using the through-the-lens viewfinder. Final alignment was accomplished by observing the camera output on an oscilloscope and adjusting the vertical camera position to place the maximum measured light level, which occurs where the beam first enters the flowfield, at the first photodiode.

To facilitate the rapid determination of actual injectant dye concentrations a calibration cell was constructed. This cell allowed the passage of a laser beam through a cavity in which a fluid, either the injectant or water from the flow loop, was flowing. By measuring the attenuation of a laser beam (usually the 496.5 nm beam from the argon-ion laser) as it passes through the cell, the dye concentration of the fluid could be accurately determined. The attenuation measurement was performed using a Lexel Model 504 laser power meter. The dye concentration of the injectant was determined prior to the experiment using the calibration cell. The dye concentration of the channel water was then continuously monitored during the course of the experiment.

Since there was a small amount of ripple in the laser light intensity level (about one percent at a frequency of about 50 Hz), the beam was sampled before entering the test section and a photodiode was used to monitor the laser intensity. The signal from this photodiode was sampled and stored with each scan of the photodiode array in the camera. This information was used to correct all fluorescence measurements for fluctuations in the excitation source intensity.

Three separate measurements with the photodiode array were required for each data set acquired. The first was a dark-level measurement in which 1000 scans of the array were digitized with the lens aperture covered and then the average dark-level voltage for each element was calculated and stored. Simultaneously, the dark level for the beam-sampler photodiode was measured and the information was stored. Next, the fluorescence intensity resulting from the presence of dye in the channel water was measured with the camera and the dye concentration of the water in the flow loop was determined using the calibration cell. These measurement allowed calculation of the constants relating the voltage from each element of the photodiode array to the dye concentration in the field of view. Finally, the fluorescence intensity was measured during injection with the photodiode array. These steps were repeated at each streamwise location and for the different fluids injected.

RESULTS

Concentration measurements were made at a Reynolds number of 42,800 based on mass-averaged velocity and channel height. This resulted in a wall-shear velocity of 3.28 cm/s and a shear rate of 1181 sec^{-1} at the wall. The primary injectant was a 700 ppm aqueous solution of SEPARAN AP-273. This polymer solution was injected at both the top and bottom channel walls at a flow rate equal to the mass flow rate through the linear portion of the viscous sublayer of the undisturbed channel flow. At these conditions, this additive yielded 28 percent drag reduction in the region from 50 to 150 mm downstream of the injector and a peak drag reduction level of 44 percent in the region from 150 to 250 mm. For the purpose of comparison, measurements were also made with injection of plain water at the same flowrate. The injected polymer solution was given an initial dye concentration of 2.05 ppm and the water was dyed at a concentration of 1.84 ppm.

For these measurements the x-axis was defined to be positive in the flow direction with its origin at the center of the injector slot. The y-axis was normal to the flow direction and normal to the long (57.5 cm) wall of the channel with its origin located at the lower wall. The x-y plane was located at the mid-span of the channel. For these measurements the excitation laser beam entered the channel through the bottom wall and passed through the flow field parallel to the y-axis.

Measurements were made at locations 10, 25, 50, and 100 mm downstream of the injector ($x^+_w = 360, 900, 1800$ and 3600 respectively). For polymer injection the first one hundred elements of the photodiode array were sampled resulting in concentration profiles which covered 6.05 mm of the flow starting at the lower channel wall. This

captured the portion of the flow with non-zero injectant concentration at all four measurement stations. For water injection measurements, this was expanded to include 150 elements (9.08 mm) at the two downstream locations.

3.1 Mean Concentration Profiles

Figures 3 through 7 show a comparison of mean concentration profiles for polymer injection and water injection at the four measurement stations. The profiles are normalized with the injection concentration, C_i , and are plotted versus distance from the wall normalized with the kinematic viscosity and shear velocity of the water flow without injection. At $x=10$ mm (Figure 3) the concentration at the wall for water injection is about 85 percent of the wall concentration for polymer injection. The apparent concentration boundary layer thickness is about $y^+ = 90$ for both flows. The obvious difference in area under the two curves indicates that the velocity in the near-wall region of the flow with polymer injection has been retarded. This agrees with observed behavior in fully developed polymer flows. Although the water injectant appears to mix more readily with the flow than the polymer solution, the wall concentrations at this location are close enough in value to indicate that the initial mixing is not strikingly different for the two injectants.

Figure 4 shows that for water injection, the wall concentration has been reduced by more than half, from 0.65 to 0.30, from $x=10$ mm to $x=25$ mm indicating rapid mixing of the injected water into the flow. For polymer injection, the wall concentration has decreased by only fifteen percent between the two stations. In the water injection flow, the injectant has reached y^+ of 130 but the polymer solution

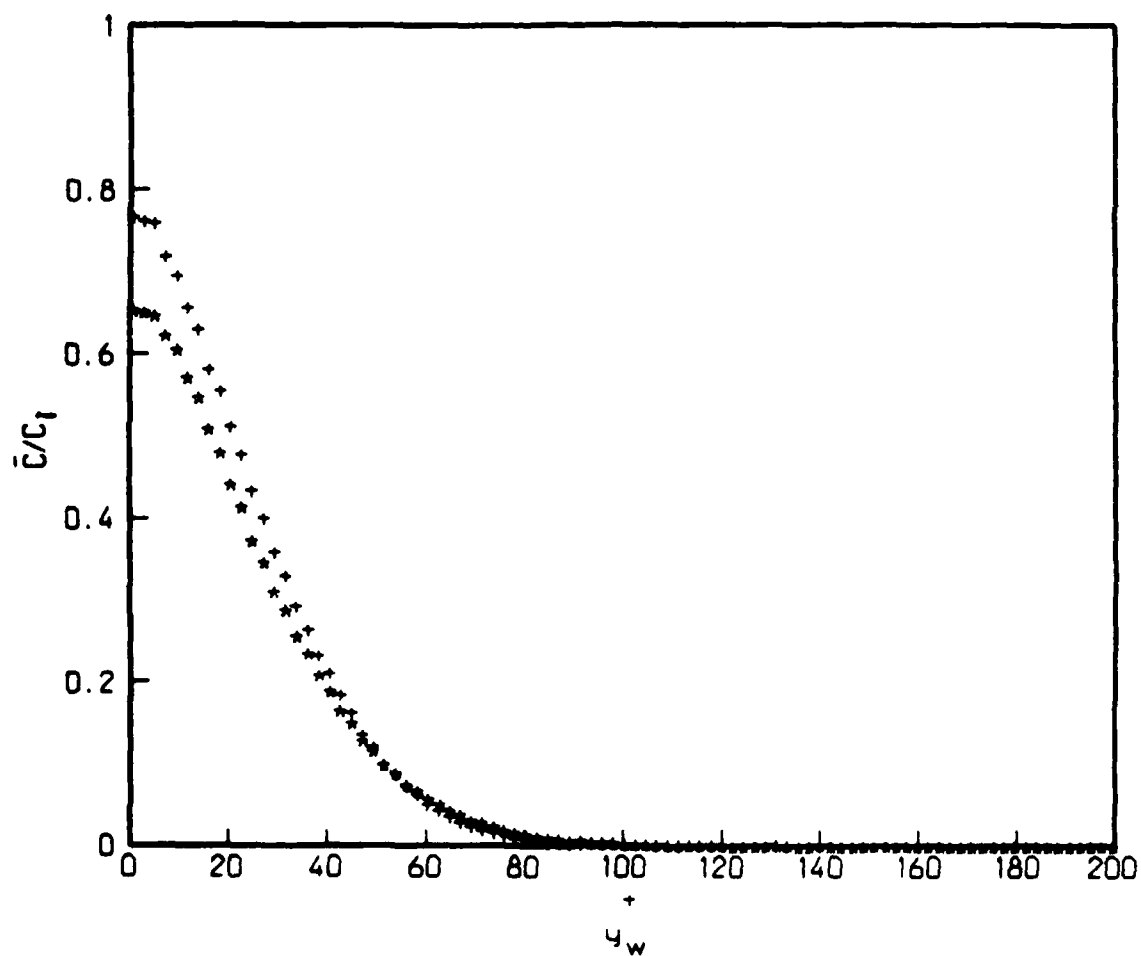


Figure 3 Comparison of mean concentration profiles at $x=10$ mm; + , 700 ppm SEPARAN AP-273; * , water.

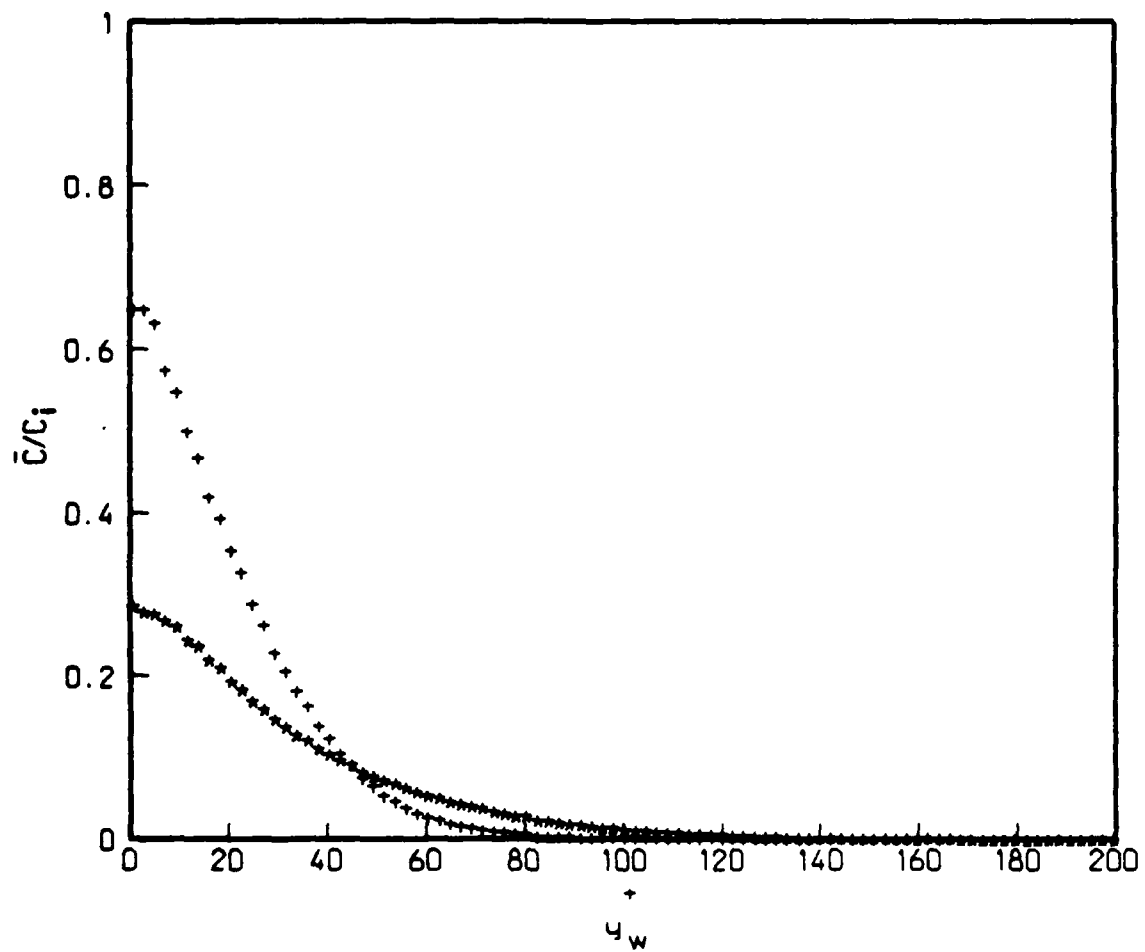


Figure 4 Comparison of mean concentration profiles at $x=25$ mm; + , 700 ppm SEPARAN AP-273; * , water.

remains confined to y^+ less than 90.

At the next measurement location, $x=50$ mm (Figure 5), except for a slight decrease in wall concentration the mean concentration profile for polymer injection is virtually unchanged from that at $x=25$ mm. This is evidence of a polymer-induced suppression of turbulent mass transport between these two measurement stations. For water injection, the wall concentration is reduced again by half and the injectant is present out to y^+ of 200.

At the last measurement station, shown in Figure 6, the wall concentration for water injection decreases by half again, and there is an appreciable injectant concentration across the entire region shown. With the polymer solution as the injectant, suppression of the mass transport has decreased as indicated by the fifteen percent reduction in wall concentration from that of the previous location and the growth of the polymer containing layer out to a distance of y^+ of 140.

3.2 Root-Mean-Square Concentration Profiles

Figure 7 shows the root-mean-square (RMS) concentration, c' , as a function of y^+ for both injectants at the first measurement location, $x=10$ mm. The RMS of the injectant concentration for water injection exceeds that of polymer injection across the flow. This is indicative of the increased mixing with water injection. With polymer as the injectant, the RMS of the injectant concentration approaches zero at the edge of the high concentration layer ($y^+ = 90-100$). This indicates that there is a small degree of mixing occurring at the interface between the polymer containing layer and the outer flow.

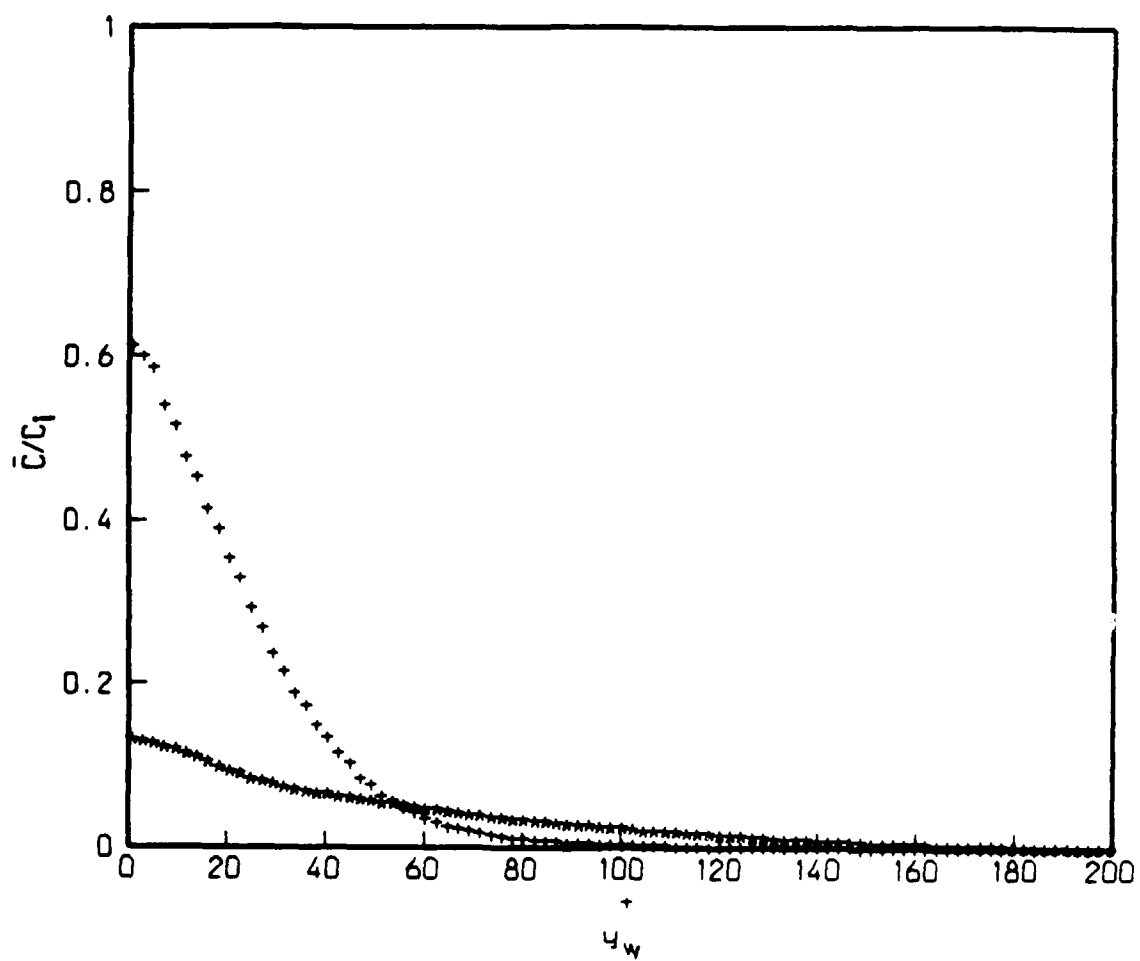


Figure 5 Comparison of mean concentration profiles at $x=50$ mm; + , 700 ppm SEPARAN AP-273; * , water.

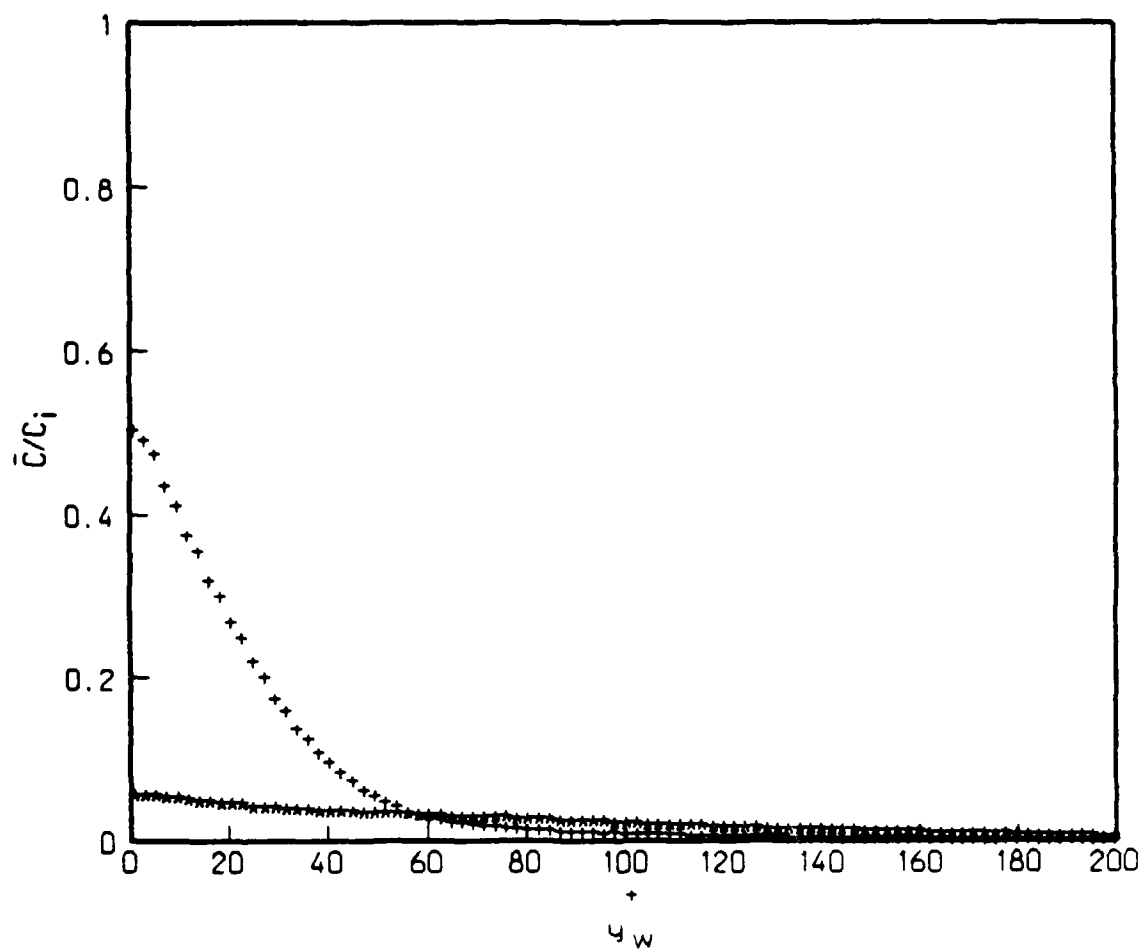


Figure 6 Comparison of mean concentration profiles at $x=100$ mm; + , 700 ppm SEPARAN AP-273; * , water.

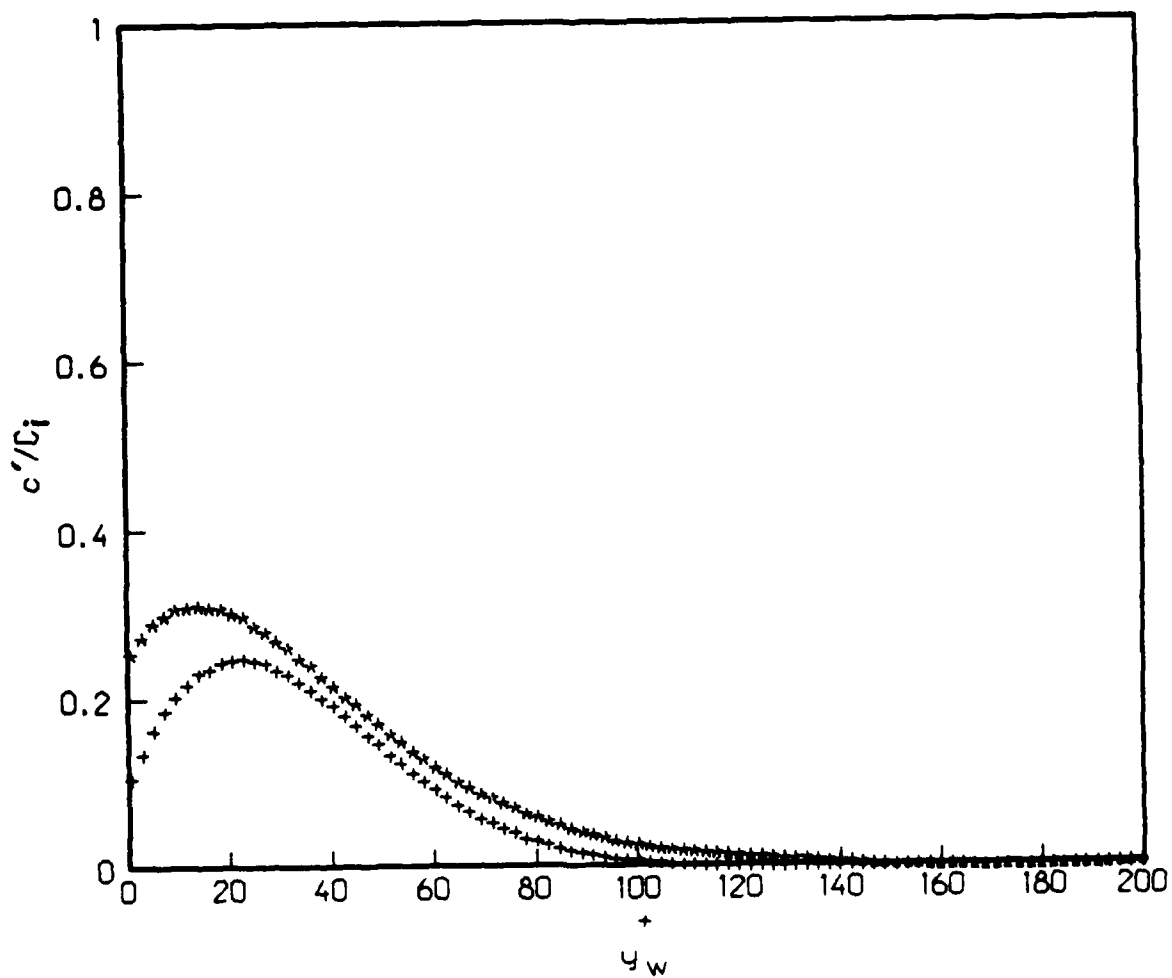


Figure 7 Comparison of RMS concentration profiles at $x=10$ mm; + , 700 ppm SEPARAN AP-273; * , water.

At the next streamwise location, $x=25$ mm, the fluctuation level has decreased near the wall for both injectants (Figure 8). For water injection the peak in c' has decreased and the curve has broadened reaching zero further from the wall. The peak value of c' for polymer injection has moved closer to the wall and the peak fluctuation level exceeds that of the water injection case. As at the $x=10$ mm measurement station, the fluctuation level approaches zero at the edge of the high concentration layer indicating that there is still minimal mixing between this wall layer and the outer region. However, the reduced fluctuation level near the wall shows that the concentration in the high-concentration layer is more uniform than at the upstream station.

Figures 9 and 10 show the RMS injectant concentration profiles for the measurement stations at $x=50$ mm and 100 mm respectively. For water injection the peak in c' continues to decrease and move away from the wall with increasing streamwise distance. At these locations the peak in c' for polymer injection is comparable to that at $x=25$ mm. Increase in values of c' further from the wall and significantly beyond the edge of the high-concentration wall layer is evidence of increased mixing between the inner and outer layers compared to the upstream positions. This increased mixing results in the decrease in near-wall concentration from $x=50$ mm to $x=100$ mm.

3.3 Time-Resolved Concentration Profiles

Time resolved measurements of injectant concentration profiles are presented in Figures 11 and 12. These data were acquired at the third measurement station

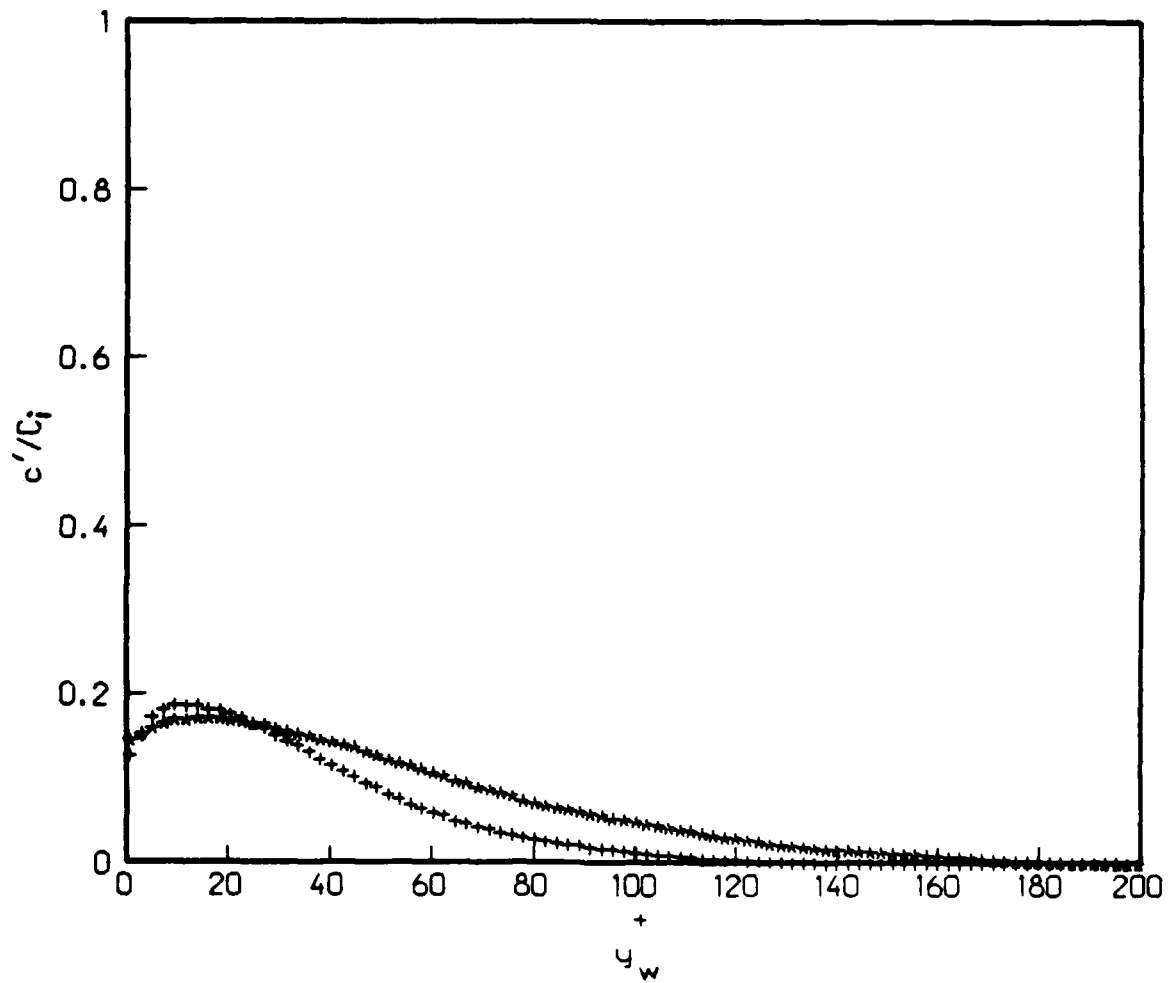


Figure 8 Comparison of RMS concentration profiles at $x=25$ mm; + , 700 ppm SEPARAN AP-273; * , water.

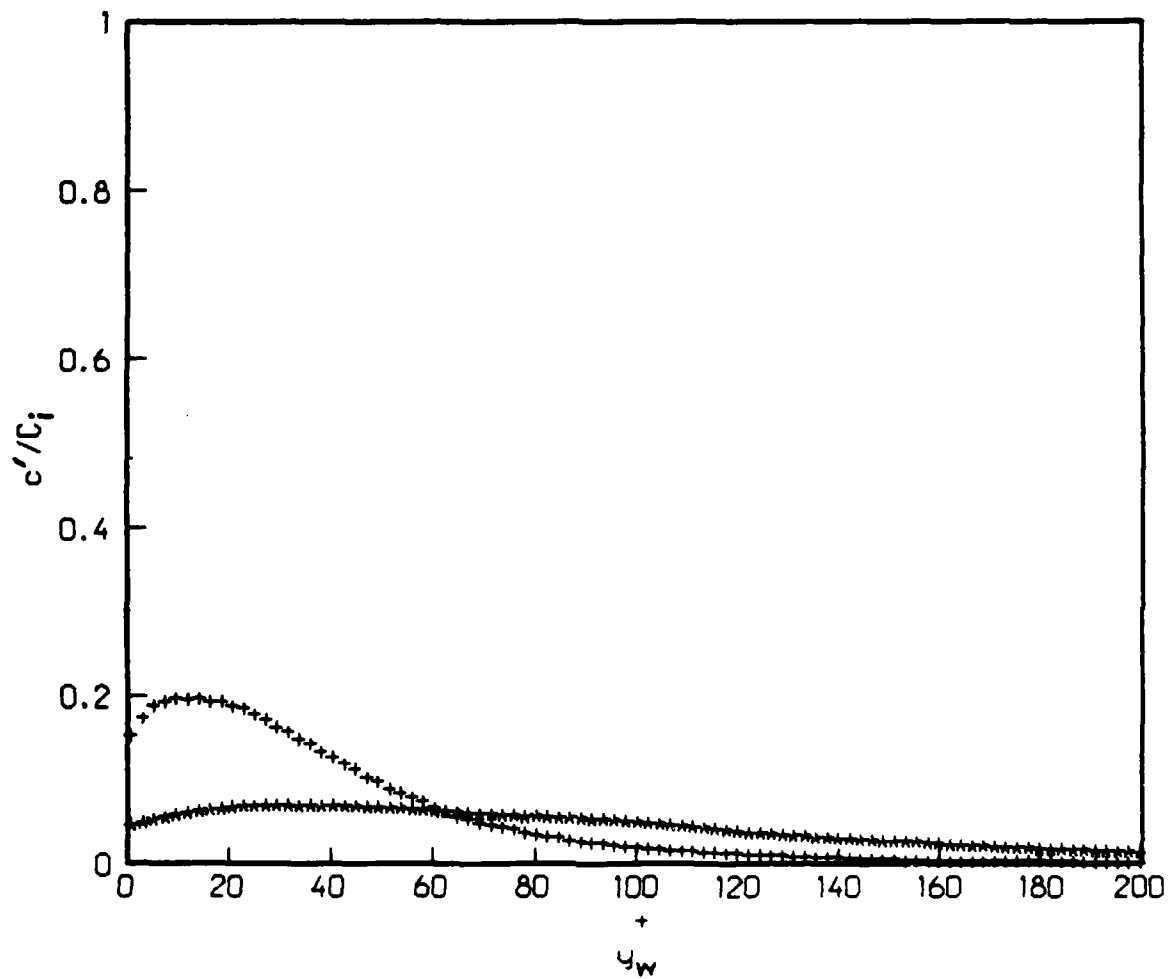


Figure 9 Comparison of RMS concentration profiles at $x=50$ mm; + , 700 ppm SEPARAN AP-273; * , water.

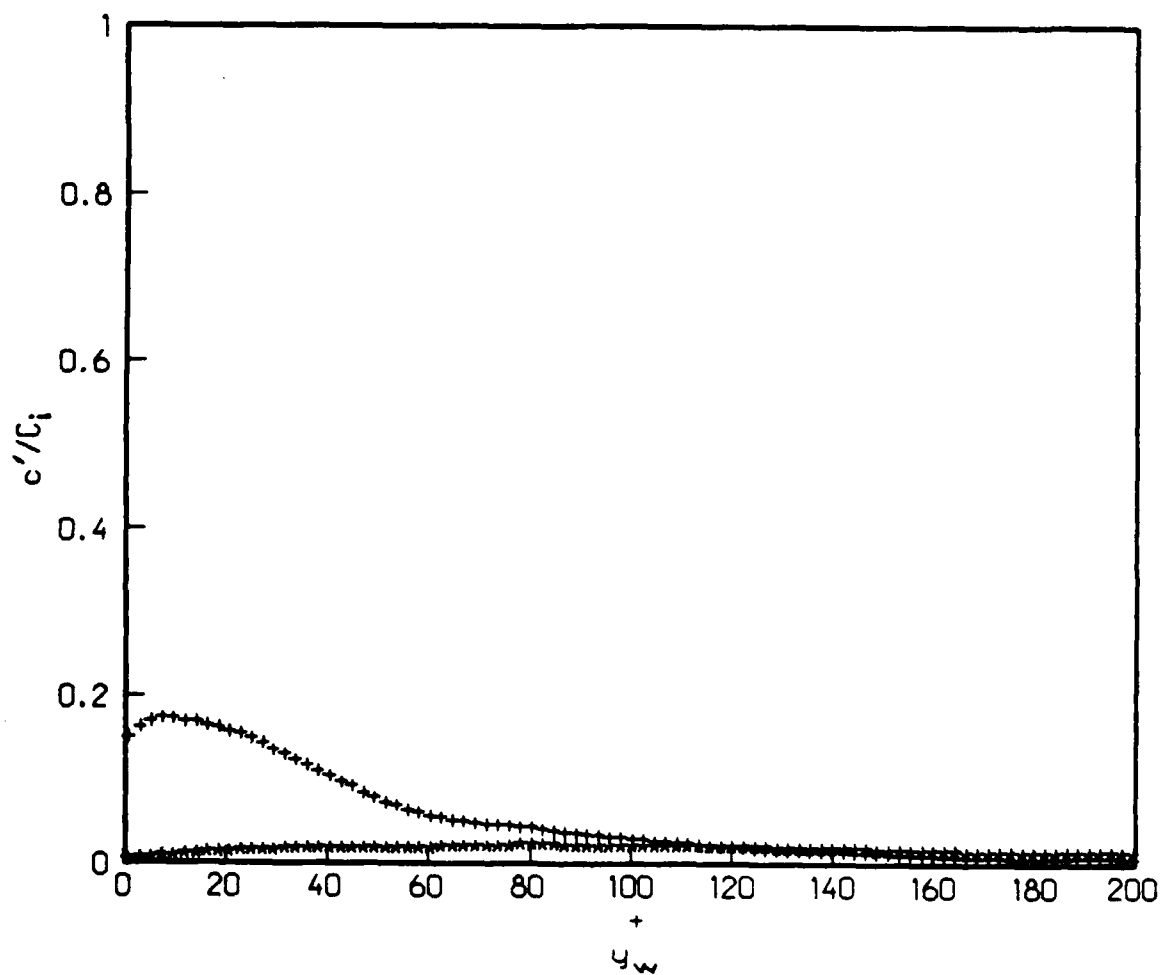


Figure 10 Comparison of RMS concentration profiles at $x=100$ mm; + , 700 ppm SEPARAN AP-273; * , water.

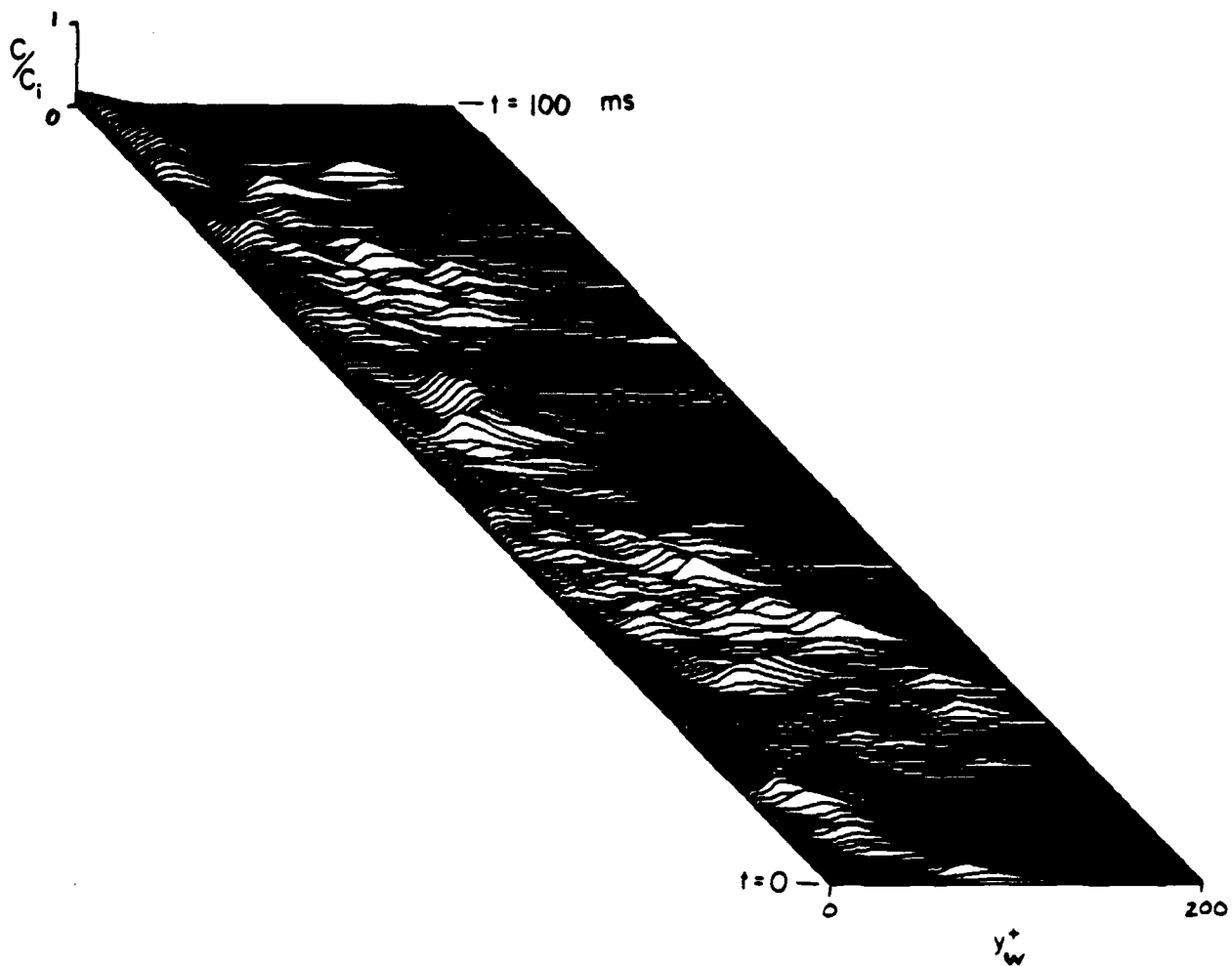


Figure 11 Time-resolved concentration profiles at $x=50 \text{ mm}$ for water injection.

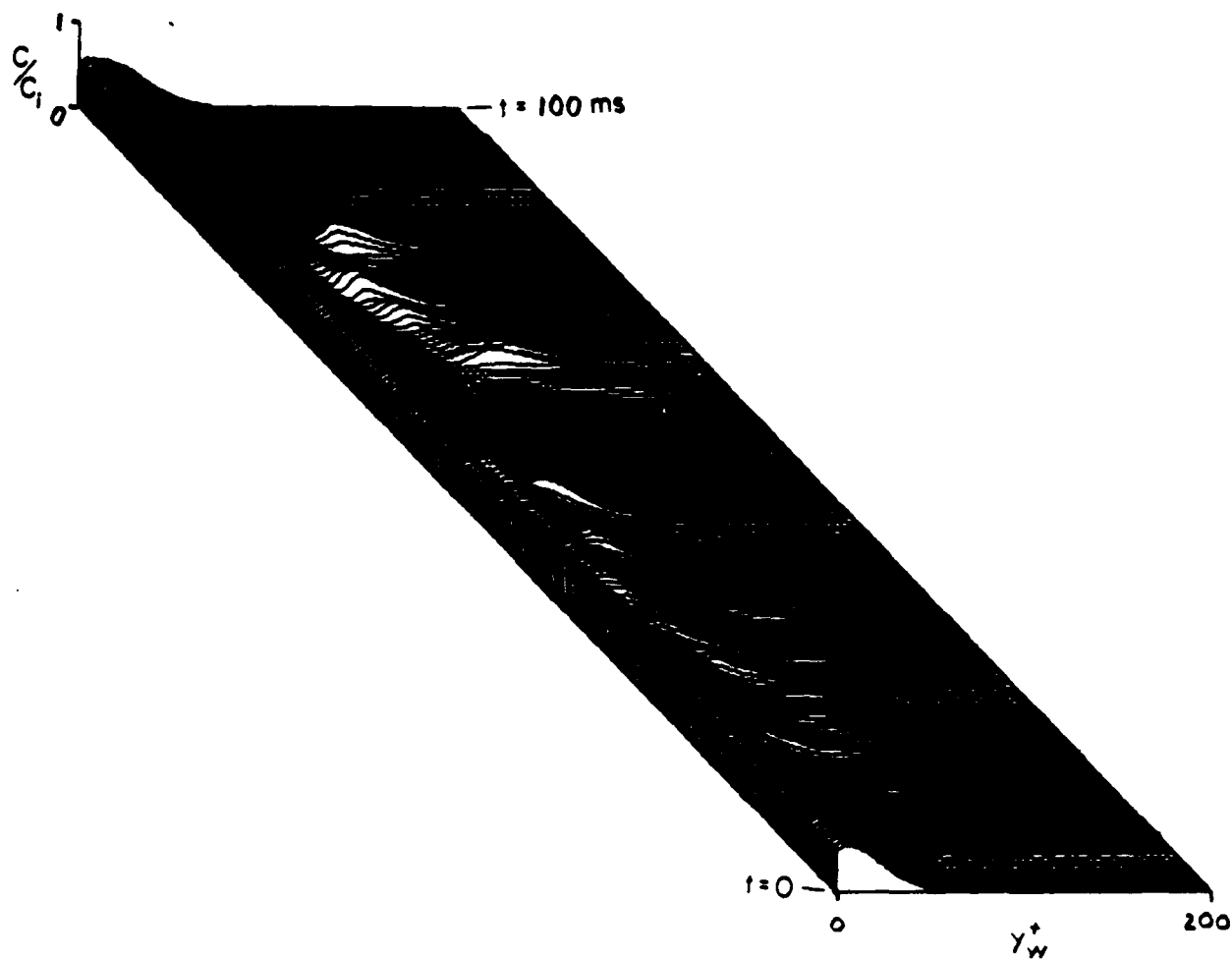


Figure 12 Time-resolved concentration profiles at $x=50$ mm for injection of 700 ppm SEPARAN AP-273.

($x=50$ mm) at a rate of two thousand profiles per second ($\Delta t = 500 \mu\text{sec}$).

Results for water injection are shown in Figure 11 for a time period spanning 100 ms. The trajectory, in time, of the high concentration regions indicates that high concentration fluid lifts away from the wall in filaments which rise near their downstream end and remain near the wall at their upstream end. The rate at which the fluid moves away from the wall is smaller than the convection velocity of the structure. Hence from the standpoint of a stationary probe, the filaments of high concentration fluid appear to move closer to the wall with increasing time. For this water injection, there is a great deal of activity across the entire region shown, and the dye filaments are highly convoluted and their passage is closely spaced in time. Figure 12 shows instantaneous concentration profiles measured over a period of 100 ms during the injection of the polymer solution. The wall concentration is relatively high and again there is evidence of periodic lifting of filaments of high polymer concentration fluid away from the wall and into the outer flow. There is a marked decrease in activity in the flow compared to the water flow. The filaments of high concentration fluid are much more distinct and widely spaced in time although they appear to extend a comparable distance from the wall.

CONCLUSIONS

The similarity in wall concentrations and apparent concentration boundary layer thickness at the first measurement station indicate that the mixing processes are comparable for the different injectants in the region $x < 10$ mm. For water injection, the near-wall concentration decreases in inverse proportion to the streamwise distance, however with polymer injection, the wall concentration decreases much more slowly and the diffusion is virtually halted in the region from $x = 25$ mm to 50 mm.

For water injection, the peak in the RMS concentration profile broadens and moves away from the wall with increasing streamwise distance while the peak level decreases. RMS concentration profiles for polymer injection indicate that there is very little mixing at the interface between the high-concentration wall layer and the outer flow until $x = 50$ mm and the concentration within the layer becomes more uniform from $x = 10$ mm to 25 mm.

Examination of time resolved concentration profiles for the two cases at $x = 50$ mm shows that high concentration fluid moves from the near-wall region to the outer flow in the form of long filaments lifting from the wall layer. These events occur less often and the filaments appear more distinct in the polymer flow than in the water flow.

REFERENCES

- Collins, D.J. and C.W. Gorton 1976 An experimental study of diffusion from a line source in a turbulent boundary layer. *AIChE J.*, 22, p.610.
- Fabula, A.G. and T.J. Burns 1970 Dilution in a turbulent boundary layer with polymeric friction reduction. NUC Technical Publication No. 171.
- Koochesfahani, M.M. and P.E. Dimotakis 1986 Mixing and chemical reactions in a turbulent mixing layer. *J. Fluid Mech.*, 170, p.83.
- Latto, B. and O.K.F. El Reidy 1976 Diffusion of polymer additives in a developing turbulent boundary layer. *J. Hydronautics*, 10, p.135.
- Latto, B. and O.K.F. El Reidy and J. Vlachopoulos 1981 Effect of sampling rate on concentration measurements in nonhomogeneous dilute polymer solution flow. *J. Rheology*, 25, p.583.
- Latto, B. and O.K.F. El Reidy 1984 Dispersion of polymer additives in a developing turbulent boundary layer. In: Drag Reduction, R.J.H. Sellin and R.T. Moses, eds., Univ. of Bristol, p.B6.
- Walker, D.T. and W.G. Tiederman 1987 Near-field effects of polymer wall injection on turbulent channel flow. In: Proceedings of the Twentieth Midwest Mechanics Conference, W. Soedel and J.F. Hamilton, eds., Vol. 14a, pp. 71-76, Purdue University, West Lafayette, Indiana.
- Walker, D.T., W.G. Tiederman and T.S. Luchik 1986 Optimization of the injection process for drag reducing additives. *Exp. in Fluids*, 4, p.114.

DISTRIBUTION LIST

Dr. Michael M. Reischman, Code 1132F
Office of Naval Research
800 North Quincy Street
Arlington, VA 22217

Office of Naval Research
Resident Representative
536 S. Clark Street, Rm. 286
Chicago, IL 60605-1588

Director
Naval Research Laboratory
Attn: Code 2627
Washington, DC 20375
(6 copies)

Professor D.G. Bogard
Department of Mechanical Engineering
The University of Texas
Austin, TX 78712

Dr. Steve Deutsche
ARL
Pennsylvania State University
P.O. Box 30
State College, PA 16801

James H. Green, Code 634
Naval Ocean System Center
San Diego, CA 92152

Professor T.J. Hanratty
Department of Chemical Engineering
1209 West California Street
Box C-3
Urbana, IL 61801

Dr. R.J. Hansen, Code 1215
Office of Naval Research
800 North Quincy Street
Arlington, VA 22217

Defense Technical Information Center
Building 5, Cameron Station
Alexandria, VA 22314
(12 copies)

Mechanical Engineering Business Office
Purdue University
West Lafayette, IN 47907

Dr. O. Kim, Code 6124
Naval Research Laboratory
Washington, DC 20375

Professor S.J. Kline
Thermosciences Division
Department of Mechanical Engineering
Stanford University
Stanford, CA 94305

G. Leal
Department of Chemistry and
Chemical Engineering
California Institute of Technology
Pasadena, CA 91125

Justin H. McCarthy
Code 1540
David Taylor Naval Ship R&D Center
Bethesda, MD 20084

Professor E.W. Merrill
Department of Chemical Engineering
Massachusetts Institute of Technology
Cambridge, MA 02139

E.W. Hendricks, Code 4420
Naval Research Laboratory
Washington, DC 20375

Dr. J.H. Haritonidis
Room 37-461
Massachusetts Institute of Technology
Cambridge, MA 02139

Dr. D.L. Hunston
Polymer Sciences & Standards Division
National Bureau of Standards
Washington, DC 20234

Mr. G.W. Jones
Code 55W3
Naval Sea Systems Command
Washington, DC 20362

Dr. John Kim
M.S. 202A-1
NASA - Ames Research Center
Moffett Field, CA 94035

Dr. C.L. Merkle
Department of Mechanical Engineering
Pennsylvania State University
State College, PA 16801

Dr. T.E. Pierce
Code 63R31
Naval Sea Systems Command
Washington, DC 20362

Steve Robinson
M.S. 229-1
NASA - Ames Research Center
Moffett Field, CA 94035

Professor W.W. Willmarth
Department of Aerospace Engineering
University of Michigan
Ann Arbor, MI 48109

END
DATE
FILMED

5-88
DTIC